Title

Discovery of small molecules through pharmacophore modeling, docking and molecular dynamics simulation against Plasmodium vivax Vivapain-3 (VP-3).

Journal

Trials in Vaccinology, 4(5)

ISSN

2405-8440

Authors

Saddala, Madhu

Adi, Pradeepkiran

Publication Date

2018-05-01

DOI

10.1016/j.heliyon.2018.e00612

Peer reviewed

Heliyon

ELSEVIER

Received:
6 February 2018
Revised:
29 March 2018
Accepted:
18 April 2018

Cite as:
Madhu Sudhana Saddala, Pradeepkiran Jangampalli Adi. Discovery of small molecules through pharmacophore modeling, docking and molecular dynamics simulation against *Plasmodium vivax* Vivapain-3 (VP-3).
Heliyon 4 (2018) e00612.
doi: 10.1016/j.heliyon.2018.e00612

Discovery of small molecules through pharmacophore modeling, docking and molecular dynamics simulation against *Plasmodium vivax* Vivapain-3 (VP-3)

Madhu Sudhana Saddala [a,b,*], **Pradeepkiran Jangampalli Adi** [c]

[a] *Centre for Agricultural Bioinformatics, ICAR-IASRI, New Delhi, India*

[b] *Johns Hopkins University School of Medicine, Baltimore, MD, USA*

[c] *Sri Venkateswara University, Tirupati, 517502, Andhra Pradesh, India*

[*] Corresponding author.

E-mail address: msaddal1@jhmi.edu (M.S. Saddala).

Abstract

Vivapain-3(VP-3) protein is a family of cysteine rich proteases of malaria parasite is extensively reported to participate in a range of wide cellular processes including survival. VP-3 of plasmodium recognized as an attractive drug target in vector-borne diseases like malaria. In the present study we robust a homology model of VP-3 protein and generated the pharmacophore based models adapted to screen the best drug like compounds from PubChem database. Our results finds the fourteen best lead molecules were mapped with core pharmacophore features of VP-3 and top hits were further evaluated by molecular dynamics simulation and docking studies. Based on the molecular dynamics simulation and docking results and binding vicinity of ligand molecules, top five i.e., CID 74427945, CID 74427946, CID 360883, CID193721 and CID 51416859 showed the best docking scores with good molecular interactions against VP-3. Furthermore *in silico* ADMET and *in vitro* assays clearly exhibited that out of five three CID74427946, CID74427945 and CID360883 ligand molecules showed the best

https://doi.org/10.1016/j.heliyon.2018.e00612

promising inhibition against VP-3. The present study believed to provide significant information of potential ligand inhibitors against VP-3 to design and develop the next generation malaria therapeutics through computational approach.

Keywords: Pharmaceutical science, Computational biology, Molecular biology, Structural biology

1. Introduction

Plasmodium vivax is one of the devastating protozoan parasite normally infect humans (Naing et al., 2014). The *Plasmodium vivax* protozoal infection is globally burden and wide unfolding illness remains continually. The encumbrance of this protozoal infection within the world has been calculated at nearly 70−80 million people were annually infected (Carlton, 2003; Rawat et al., 2011). The *Plasmodium vivax* has persisted restrained so far, and because of many factors impending primarily relocation of people, poor sanitation, overcrowded populated countries especially middle and low income tropical countries. A special focus on dissimilar vivax strains and owing to fast resistance growth to existing antiprotozoal as well as antimalarial drugs tend to develop new targets to eliminate the malaria through drug discovery approaches (Fryauff et al., 1998; Ruebush et al., 2003). Thus, there's associate imperatively must be compelled to determine along with distinguish inventive targets for drug design to treat protozoal infection. Anti-proteases are well known dependable drugs of the hemoglobin hydrolysis, which inhibits parasite growth and survival are available in the present market (Bonilla et al., 2007a,b). Only plasmodial proteases are engaging targets for new antiprotozoal therapy in recent times, the new two cysteine rich proteases from *P. vivax* particularly, vivapain-2 and vivapain-3 (VP-2 and VP-3), are known furthermore characterized (Na et al., 2004). Both VP-2 and VP-3 share quite sequence identity with one another moreover like their evident orthologs, falcipain-2 and falcipain-3. The falcipains, the vivapains conjointly need tumbling circumstances for action, comprise acidic hydrogen ion concentration (pH) optima as well as hydrolyze substrates with stimulating amino acid residues at P1 and Leu at P2 supported their ability to hydrolyze resident hemoglobin (Hb) at sour pH concentration along with the blood corpuscle membrane proteins. The vivapains seem to possess like organic roles toward the falcipains and the degradation of hemoglobin may be an extremely ordered process (Gluzman et al., 1994). The present understanding of this process is that hemoglobin is processed within the food vacuole where it is digested into small peptides. The small peptides were after delated into the cytosol, where further dispensation of the globin fragment into free amino acids takes place. Based on the machanism, and biochemical evaluation of the parasite biology has resulted in the observation that aspartic (Francis et al., 1997), cysteine (Shenai et al.,

https://doi.org/10.1016/j.heliyon.2018.e00612

2000; Sijiwali et al., 2001) and metallo proteases (Eggleson et al., 1999) are involved in the digestion of hemoglobin in an orderly fashion. Each the falcipain moreover, because the vivapains must to be thought of upcoming therapeutic agents embattled alongside plasmodial cysteine proteases.

The vivapains are plasmodial proteases to *Plasmodium vivax*. Its genes predicted papain-family cysteine proteases, which shared a few unusual features with falcipains, including large pro-domains and short N-terminal extensions with catalytic domain, which are similar biological roles to the falcipains.

The cysteine rich family protease of *P. falciparum* plays an important role in the parasite life cycle by degrading erythrocyte proteins, most notably hemoglobin. Inhibition of FPs is a challenging task for parasite maturation, may be appreciated targets for the design of novel antimalarial drugs, but lack of protein structural knowledge impended to develop the rational discovery with selective, and efficacious inhibitors using computational approaches.

One in all the first needs to investigate a structure based drug design agenda is that the convenience of the 3D (three dimensional) structure of the objective enzyme. The non-availability crystal structure of VP-3 proteins, put urgency to develop homology modelling, with template based valid proteins, offers an affordable results and further molecular docking studies were carried out.

The high throughput computer-generated screening, structure based pharmacophore, virtual screening and molecular dynamics (MD) simulation provides a reliable information and an efficient drug discovery approach. During this contribution work elucidate the novel ligand inhibitors and molecular interactions of ligands against VP-3. The interactions of the protein−ligand, binding energy calculations, affinity predictions and validations explore the best ligand inhibitors against VP-3.

2. Materials and methods

2.1. Homology modeling

Plasmodium VP-3 sequence (Q6J109) retrieved from Uniport (http://www.uniprot.org/) database. The template structure of falcipain-3 in complex with Leupeptin (PDB ID: 3BPM) of *P. falciparum* was chosen through BLASTp analysis (Altschul et al., 1997). The homology modelling method was enforced to establish the tertiary structure of VP-3 utilize Modeller 9.13v (Eswar et al., 2008). It performs an information search by building a profile of sequences iteratively. The Clustalx was worn for key target model alignment (Thompson et al., 1997) is shown in (Supplementary data Fig. S1). The arrangement file was transformed to a modeller contribution format (PIR- super molecule data resources − *.ali) with inclusion of Leupeptin.

https://doi.org/10.1016/j.heliyon.2018.e00612

2.2. Model evaluation

The homology modelling section was followed by the model analysis section. The stereo chemical quality and structural integrity of the model VP-3 was tested by RAMPAGE server (Laskowski et al., 1993) (Fig. 1a), ERRAT (Colovos and Yeates, 1993), ProSA (Sippl, 1993; Wiederstein and Sippl, 2007) and Verify3D (Bowie et al., 1991; Luthy et al., 1992) softwares and the target−template superimposition is shown in (Fig. 1b) (Eswar et al., 2008).

2.3. Pharmacophore design

The modelled structure of VP-3 in complex with an inhibitor Leupeptin was worn as beginning structure for the construction of pharmacophore models. Ligandscout v3.10 (LS) could be an apparatus that permits the automated construction in addition to apparition of 3D pharmacophore as of structural knowledge of macromolecules/inhibitor complexes (Wolber and Langer, 2005). As for the LS rule, compound options embody hydrogen bond donors (HBD) and acceptors (HBA) as focussed vectors along with negative and positive ionizable spheres furthermore as lipophilic regions are illustrate by spheres. Additionally, to extend the electivity, the LS representation merge spatial data concerning regions unattainable to every prospective inhibitor, so reflective attainable steric restrictions. Specifically, expelled level regions located in positions that are sterically out are mechanically supplementary towards

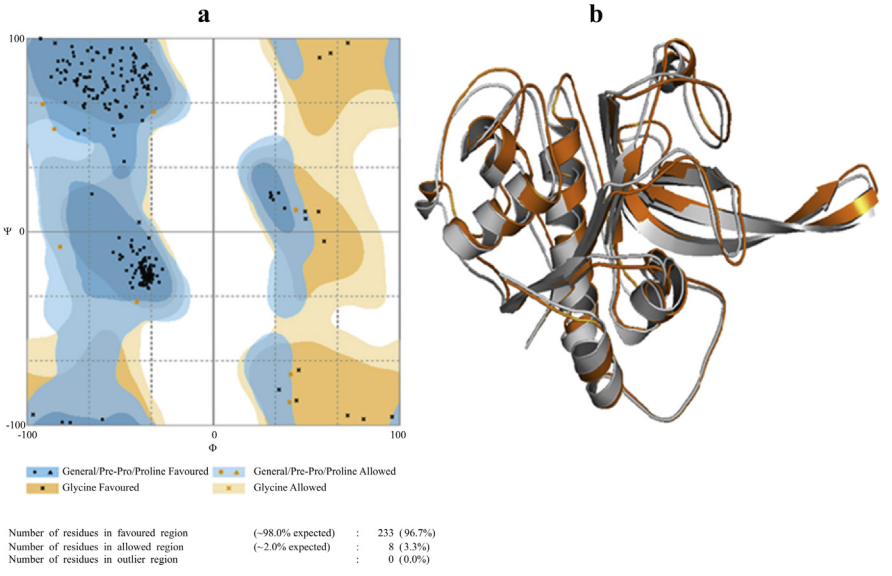

Fig. 1. 3D model structural assessment of the VP-3 protein (a). Ramachandran plot shows 96.7% of residues were found in the favored region (blue), 3.3% in the allowed (yellow), and none in the outlier regions (white). (b). Modelled 3D structure of protein VP-3 superimposition of the (orange) and template 3D structure of falcipain-3(white) (PDB: 3BPM).

https://doi.org/10.1016/j.heliyon.2018.e00612

the designed pharmacophore model. The LS tool was practical to the recognition and investigation of decisive contact patterns amid VP-3 and Leupeptin.

2.4. Virtual screening

Leupeptin, conjointly referred to as N-acetyl-L-leucyl-L-leucyl-L-argininal, represents a best anti-protease agent that may inhibit cysteine, serine and threonine peptidases. The serine proteinases (trypsin (Ki = 3.4 nM), plasmin (Ki = 3.5 nM), porcine kallikrein), and cystein proteinases (papain, cathepsin B (Ki = 4.1 nM), endoproteinase Lys-C) are inhibited (Maes et al., 2007). The structure of Leupeptin (CID72429) along with its analogous were taken in a SDF (Structure data format) from a PubChem database (http://pubchem.ncbi.nlm.nih.gov/), an unwrap storehouse for small compounds. All the compounds were initially energy minimization done by the Open Babel in PyRx Virtual Screening Tool (Dallakyan, 2008). Once consider the pharmacophore query, virtual screening was passed out by the LS next to the PubChem database. The known hits, were docked into the receptor with known binding pocket of VP-3.

2.5. Molecular docking

Molecular docking studies was carried out by the AutoDock 4.2 (Morris et al., 2009) in PyRx Virtual Screening Tool (Dallakyan, 2008) was utilized to come up with the docking key files. Experiential free energy utility and Lamarckian genetic algorithm (LGA) amid the consequent settings: at most numeral of 2,500,000 energy evaluations, a preliminary population of one hundred fifty indiscriminately placed individuals, at most numeral of 27,000 generations, a transmutation rate of 0.02, a crossover velocity of 0.8, along with an exclusiveness rate (numeral of top individuals to endure to next generation) of one were designed for docking. The supposed Solis and Wets law was useful to a most of three hundred iterations for each look for confined search. The default principles were thought of designed for all the previous parameters not mentioned.

2.6. Refinement of homology model

The lead compounds were parameterized by the SwissParam module for MD simulations. SwissParam could be a quick field of force generation apparatus for tiny compounds (SwissParam, http://www.swissparam.ch). It generates parameters that are according to the CHARMM27 field of force (for energy minimization). Ions and water were generated by VMD 1.9.1(Visual Molecular Dynamics) (Humphrey et al., 1996). The counter ions were positioned for neutralization and TIP3P (Transferable Intermolecular Potential 3P) waters were positioned at arbitrary. The extent of hypothesis worn was HF/6-31G (d) (Hartree-Fock/6-

https://doi.org/10.1016/j.heliyon.2018.e00612

31Gaussian), and was according to different QM/MM (Quantum Mechanics/Molecular Mechanics) ways (MacKerell et al., 1998).

2.7. Molecular dynamic simulations

The molecular dynamic (MD) simulation of VP-3 was done by NAMD 2.7 (Nanoscale Molecular Dynamics) with the CHARMM27 field of force and the on top of mentioned parameterized compounds to be used during this field of force (Brooks et al., 1983; Laxmikant et al., 1999; Pradeepkiran et al., 2015). All VP-3 MD simulations were encompassed of a water small package restrain about 29,000 TIP3P water molecules that were supplementary round the VP-3 to produce a deepness of 11−13 Å as of the sting of the particle (Jorgensen et al., 1983). The ionic concentration used for the MD simulations is 0.145 M. These steps were sprint by neutralizing counter ions. These were positioned by the VMD plug-in module (Humphrey et al., 1996). We have a tendency to use the subsequent VdW (Van der Waals) parameters for Na^+: radius 1.868 Å and a fit deepness of 0.00287 kcal/Mol (Ross and Hardin, 1994). Simulations were encountered away by the PME (particle mesh Ewald) technique with recurrence margin surroundings during a small package about 4.4 × 105 Å3 (dimensions: 90 Å × 70 Å × 70 Å) with 9 Å non-bonded cutoff (Darden et al., 1993) by SHAKE through a 2-fs point in time step (Ryckaert et al., 1977). Pre-equilibration was on track with 10,000 steps of minimization go after by 2 ns of warm up underneath MD with fetters on the atomic arrangement of compounds and VP-3. Subsequently, three rotation of minimization (5000 steps each) and warm up (1 ns) were meted out with restraints of 10, 5 and 0.5 kcal/ (Mol Å2) applied to the VP-3 and lead compounds. This was pursue by 1 ns of deliberate warm up with NPT MD, wherever the arrangement was gradually warm up from one to 310 K, with insignificant moderation pertain within the five VP-3 and ligand complexes (0.01 kcal/(Mol $Å^2$)). Subsequent warm up, the arrangement warmth was re-scaled more following 3.4 ns by NVT with Langevin thermostat by NAMD procedure (Izaguirre et al., 2001; Phillips et al., 2005). After this, we have tendency to think about the arrangement at the production-level designed for MD steps. An NPT force and stable hotness of 310 K was sustained by the Berendsen weak-coupling regulation with a moment stable of 1.0 ps and NVT ensemble ways (Izaguirre et al., 2001; Berendsen et al., 1984). Our technique of arrangement, warm up, stabilization and construction is comparable to recognized procedures within the literature (Reblova et al., 2006; Spackova and Sponer, 2006). The binding free energy calculations revealed the modifications of binding affinity between dissimilar ligands and the binding pocket. The methods like MM/PBSA43 and MM/GBSA44 are generally used to exploring the energetic contribution of protein−ligand binding affinities. For different protein−ligand systems, the process of converged status was used for the binding free energy computation. The solute and solvent dielectric constants were set at 1. 0 and 60.0 and the binding free energy

https://doi.org/10.1016/j.heliyon.2018.e00612

(Cunha et al., 2004) of various lead compounds to the VP-3 was calculated as follows:

$$\Delta G_{binding} = G_{complex} - [G_{protein} + G_{ligand}].$$

For different protein−ligand systems, the process of binding free energy calculations was also applied to hydrogen bond occupancy calculations. The hydrogen bond distance was set at 3.5 Å and the angle was 120.0°. The other parameters were kept default.

2.8. Chemical analysis of drug-likeness

Molsoft Drug-Likeness explorer (http://www.molsoft.com/mprop/) was worn to investigate the drug-likeness as indicated by ''Lipinski Rule of 5'' (Lipinski et al., 1997). In keeping with ''Lipinski Rule of 5'' a compound is a lot of possible designate membrane permeable and merely captivated through the body if its relative molecular mass is a smaller amount than 500, its lipophilicity, expressed as an amount referred to as *Log P* is a smaller amount than five, the number of groups within the compound that may give hydrogen atoms to hydrogen bonds is a smaller amount than 5 and also the numeral of group that may settle for hydrogen atoms to make hydrogen bonds is a smaller amount than 10 (Leeson, 2012).

2.9. ADMET properties

The computational pharmacokinetic properties and absorption, distribution, metabolism, elimination, and toxicity (ADMET) were investigation through online Osiris property explorer (http://www.organic-chemistry.org/prog/peo/; Access date: September 23, 2016) uses Chou and Jurs rule, supported computed atom contributions figure out the ligands properties.

2.10. Antimalarial activity

Plasmodium vivax (*P. vivax*) was cultured according to modified method of Trager and Jensen (1976) in cord blood containing immature red blood cells (reticulocytes) at a 5% hematocrit in McCoy's 5A medium, supplemented with L-glutamine (4.2 mM), HEPES buffer (25 mM), $NaHCO_3$ (25 mM) hypoxanthine (6.8M), 0.5% Albumax II (Invitrogen) and 50 μg/ml Gentamicin (Trager and Jensen, 1976). Culture medium was earlier sterilized by filtration through a membrane filter of 0.22 μm porosity for making stock 250 ml and stored in a sterile screw capped bottle. The working media was again filtered using syringe filter, the filtrate was stored in 125 ml square bottle, sealed with parafilm and stored in refrigerator at 2−4 °C, which was ready to use. Complete McCoy's 5A medium was taken in a sterile tissue

https://doi.org/10.1016/j.heliyon.2018.e00612

culture flask and *P. vivax* species were cultivated. The inoculum was incubated at 37 °C in 5−10% CO_2 incubator.

2.11. In vitro antimalarial assay

The *in vitro* antimalarial assay was carried out according to microassay of Rieckmann and co-workers method (Rieckmann et al., 1978), with minor modifications. For this assay, the test compounds were dissolved in dimethyl sulfoxide (DMSO) and being prepared in a series of concentration such as 10, 50, and 100 μg/mL respectively and using Leupeptin as reference drug. In triplicate wells were incubated with parasitized cell preparation at 37 °C in a CO_2 incubator set at 37 °C and 5% CO_2 level. After 40 h of incubation, the blood smears were prepared from each well and stained with Giemsa stain and made it as thin blood layer. The parasitemia and the inhibition percentage of *P. vivax* growth were calculated from the number of infected erythrocytes for every 1000 erythrocytes. Based on analysis of the correlation between concentrations of the compound with the inhibition percentage was conducted using probity log analysis in order to determine the IC_{50}.

2.12. Cytotoxicity assay

PC12 (Pheochromocytoma) cell cultures were obtained from National Center for Cell Sciences (NCCS), Pune, India. Stock cells were refined in DMEM supplemented with 10% inactivated Fetal Bovine Serum (FBS), penicillin (100 IU/mL), streptomycin (100 μg/mL) and amphotericin B (5 μg/mL) in a humidified air of 5% CO_2 at 37 °C until intersecting. The cells were separated with TPVG solution (0.2% trypsin, 0.02% EDTA, 0.05% glucose in PBS). The stock cultures were developed in 25 cm^2 culture flasks and all trials were done in 96 microtiter plates. For cytotoxicity studies, each measured test compounds were independently dissolved in 10% DMSO and volume was made up with DMEM supplemented with 2% inactivated FBS to acquire a stock solution of 1 mg/mL concentration and sanitized by filtration, serial two fold dilutions were prepared from this for completing cytotoxicity studies.

In vitro development impacts of test compounds were surveyed by calorimetric method. Where the determination of transformation of MTT into Formazan blue by living cells (Dolly and Griffths, 2000). The supernatant was expelled from the plate, and after that new Hanks adjusted salt solution was added and treated with various concentrations of compounds diluted with DMSO and control group contain just DMSO. After 24 h incubation at 37 °C in a humidified atmosphere of 5% CO_2, the medium was supplanted with MTT solution (100 μg/mL, 1 mg/mL in sterile Hanks balanced solution) and kept 4 h for incubation. The supernatant painstakingly aspirated, the precipitated crystals of formazan blue were solubilized by adding DMSO (200 μg/mL) and absorbance was measured at λ 570 nm. The assay

https://doi.org/10.1016/j.heliyon.2018.e00612

can be performed totally in a microtiter plate (MTP). It is suitable for measuring cell multiplication, cell feasibility or cytotoxicity.

The concentration at which the absorbance (562 nm) of treated cells was reduced by 50% with respect to the untreated control was calculated using the following formula:

$$\text{Surviving cells } (\%) = \frac{\text{OD of the test Compound}}{\text{OD of the Control}} \times 100$$

2.13. Statistical analysis

The GraphPad prism v5.0. Statistical software used to carried out using the Kruskal-Wallis test was applied to determine the non-parametric comparisons, and the fisher test was employed to calculate statistical significance. The non-parametric correlation analysis was carried out using the Spearman correlation (r_s) model.

3. Results and discussion

One of the major objectives in the drug discovery part to spot new compound entities that encompass an elevated chance of binding to the goal macromolecule to obtain the required biological retort. For this pharmacophore based virtual screening technique is more accustomed progress the potency and effectiveness of the drug intervention (Trager and Jensen, 1976). The *Plasmodium* VP-3 (Accession no. AAP04594.1) was known as a typical drug target for malaria.

3.1. 3D-model construction and validation

In the lack of an absolute crystal structure of VP-3 in *P. falciparam*, homology modeling methods modeller gaining an important tool for constructions of 3D protein structure. Crystal structure of facipain-3 (3BPM) in composite with Leupeptin from *P. falciparam* showed maximum sequence identity (57%) with the VP-3, hence, it had been selected as a templet (Table S1). Incorporating ligand into the homology sculpt from the structural templet will increase largely exactness of the expected models (Eggleson et al., 1999) still as assists in deciding compound binding sack of the medicine goal, consequently, leupeptin was integrated into the homology sculpt from the structural templet. Total 100 models of VP-3 build using modeller programme. Based on discrete optimized protein energy (DOPE), we selected as eighteenth model showing the low energy −989.58606 attain in homology modeling. DOPE is a statistical potential used to assess homology models in protein structure prediction. DOPE is based on an improved reference state that corresponds to non-interacting atoms in a homogeneous sphere with the radius dependent on a sample native structure; it thus accounts for the finite and spherical shape of the

https://doi.org/10.1016/j.heliyon.2018.e00612

native structures. The low DOPE attain correspond to comparatively a lot of stable 3D conformation of the drug target (Eswar et al., 2008). Therefore, the eighteenth model of VP-3 with very least DOPE score was selected for MD simulation studies.

The superimposed structure of modelled protein imposed to more be similar and exactly impended the template structure shown in (Fig. 1b). To assess the stereochemical quality and structural integrity of the model, RAMPAGE, ERRAT, ProSA and Verify3D software package were used. RAMPAGE is a branch of RAPPER that engender a Ramachandran plot. It's counselled that it's used for this principle in predilection to PROCHECK, which relies on a lot of huge information. The Ramachandran plots psi versus phi dihedral angles for every amino acid within the protein. The plot is split into favoured, approved and barred area, those contouring relies on density-reliant smoothing for 81234, non- Proline Non-Glycine amino acids with $B < 30$ from 510 elevated decision protein structures. Areas are also outlined for Proline, Glycine, as well as pre-Proline as shown in (Fig. 1a). The ERRAT could be a macromolecule structure verification algorithmic program, that is, particularly well-suited for differentiating between properly and incorrectly determined regions of macromolecule structures supported characteristic atomic interactions. The program affords an "overall quality factor" assessment that is outlined because the share of the macromolecule that the considered blunder rate collapse less than the 95% statistical refusal border. The ERRAT in general excellence concern of the model is 92.340 (Fig. S2). ProSA (Protein Structure Analysis) program could be an investigative tool that's supported the geometric investigation of all accessible macromolecule structures. The power of the construction is appraised utilizing a distance-based come together prospective and a prospective that confines the solvent disclosure of macromolecule amino acids. From these power, two descriptions are derived and displayed: Z-score along with a plot of amino acid energies. The Z-score point towards overall model excellence moreover process the divergence of the total power of the structure through relevancy a power allotment imitative from arbitrary conformations. The power plot illustrates the native model excellence by plotting energies of residues in sequence (Fig. S3). In all-purpose, constructive principles keep up a correspondence to problematical or erroneous components of the model. The Verify3D profile shows for the VP-3 model structure (Fig. S4). Amino acids with a score over 0.2 ought to be thought-about consistent. Taken along, all the higher than information indicate that the standard of the model is sweet enough to be a preparative purpose for ensuing part of docking studies.

3.2. Pharmacophore design

The pharmacophore model mechanically produced by the LS tool comprises four features: 3 HBD (green), one positive ionizable group (blue) as well as one hydrophobic group (yellow) are revealed in (Fig. 2a). Spheres are within 5 Å distance from

https://doi.org/10.1016/j.heliyon.2018.e00612

the inhibitor was generated. Further, the program mechanically produced many excluded volumes (gray) within the model. The HBD description indicates toward the three amino groups of the ligand from the Tyr163, Glu216 and Gln223 correspondingly (Fig. 2b). The HBD sphere has 2.5 radius, θ: 95.27 and φ: 0.02. (Co-ordinations X: −20.85, Y: 86.42, Z: 13.58). The positive ionizable sphere has 1.3 radius, θ: 76.21 and φ: 0.42 (co-ordinations X: -19.25, Y: 67.75, Z: 32.25). The hydrophobic sphere has 1.0 radius, θ: 72.59 and φ: 0.12 (co-ordinations X: −12.25, Y: 61.32, Z: 38.68). The hydrophobic features are set within the propyl group of the ligand. Within the test database, we kept the ligand (i.e. Leupeptin) present in complex structures. First, the Leupeptin was extracted and then, hydrogen atoms were added and energy minimized by the LS. The minimized structure of Leupeptin was additional to the analysis database. When screening, the analysis compounds were properly plot by the pharmacophore model as shown in (Fig. 2c). The outcome confirmed the legality of our pharmacophore model which will be worn for the screening of enormous databases.

3.3. Pharmacophore virtual screening

The valid pharmacophore representation was then worn as computationally receive to screen the PubChem database (http://pubchem.ncbi.nlm.nih.gov/) of commercially accessible ligands. The PubChem database ligands in SDF

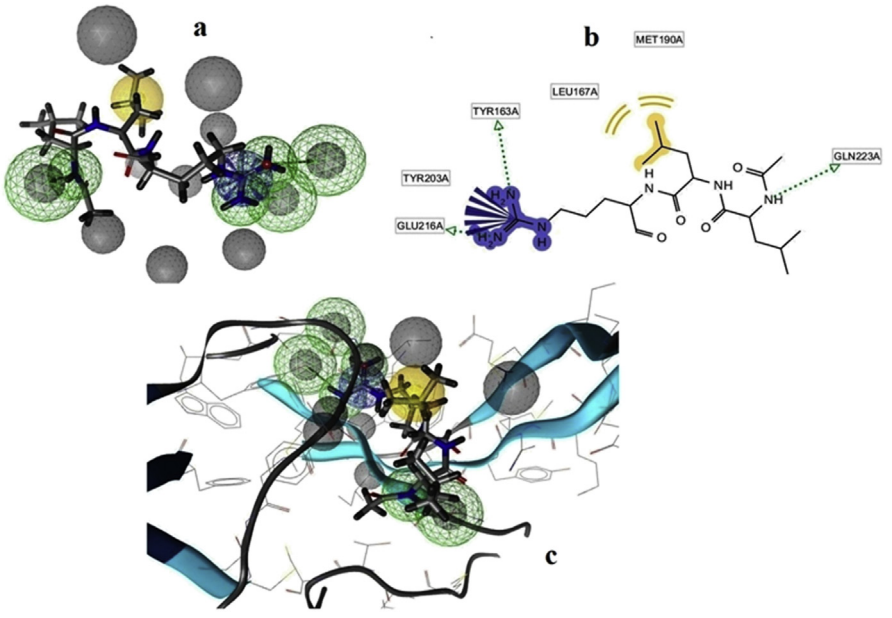

Fig. 2. The VP-3 pharmacophore model generated by LigandScout a). Three hydrogen bond donors (HBD) (green), one positive ionizable group (blue), one hydrophobic group (yellow) and excluded volumes (grey) in the model. b). The dotted arrows indicated the hydrogen bond acceptor features. c). The complex structure of VP-3 and Leupeptin of pharmacophore model.

https://doi.org/10.1016/j.heliyon.2018.e00612

configure were encumbered into LS setting wherever the 3D configuration of every ligand was modelled by the MMFF94x force field. The conformation introduce methodology was pertaining to acquire low-energy conformations for every ligand. The conformations of each ligands were then sieved by the pharmacophore model. To be thought about as hit, the ligand has got to equivalent all the features of the pharmacophore. This pharmacophore based virtual screening, 14 hits (Fig. 3) were recognized that diagram on the extended pharmacophore model (i.e. including the desired needs). These at first known hits were elite for further investigation by docking studies.

3.4. Molecular docking and dynamics

To construe the hopeful ligands for inhibitors of VP-3, all the primary hits were docked into the newly recognized binding pocket of VP-3 by the AutoDock 4.2 in PyRx virtual screening Tool. The docking simulation energies was determined for each legend with 10 exhaustiveness. Active site grid dimensions were set as X = 64.3194, Y = 42.7549 and Z = 70.365 for centre and total size dimensions were set as X = 72.7563455571, Y = 75.3566472888 and Z = 81.8179926682. Based on the AutoDock binding energies, best five leads were identified compared to the Leupeptin (query) compound. The docking results are shown in (Table 1). The

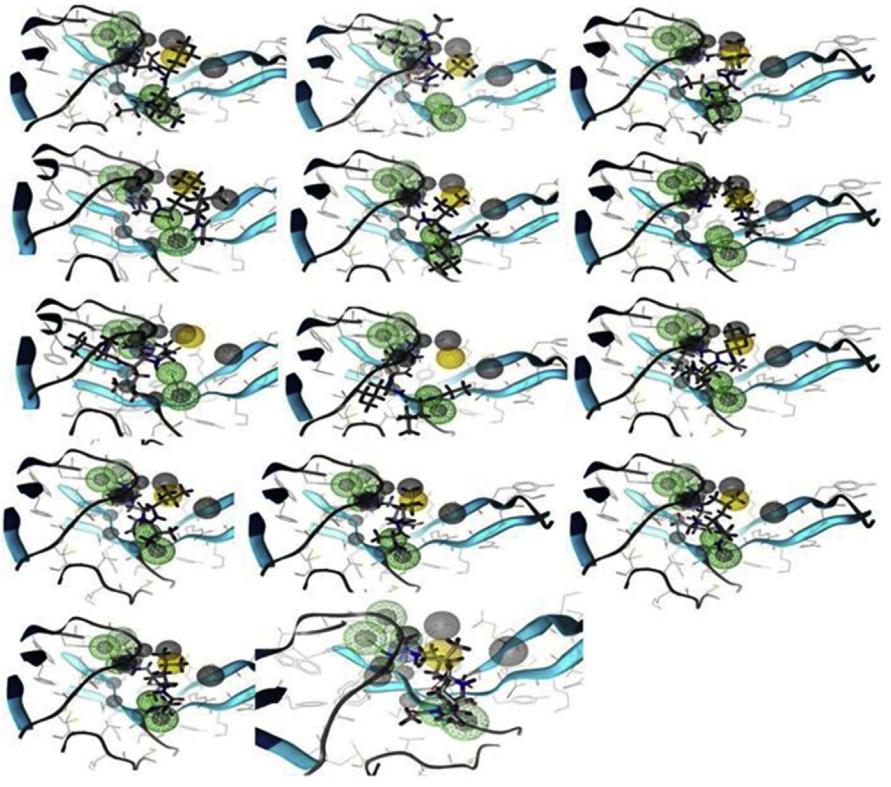

Fig. 3. Pharmacophore based virtual screening 14 hits from PubChem database.

https://doi.org/10.1016/j.heliyon.2018.e00612

compound CID 74427946 has best binding affinity (−10.8 kcal/mol). The interacted amino acid residues were GLY-85, HIS-176, SER-151 and GLN-236. The interactions were observed in all the five compounds with query compound leupeptin (Table 1). In (Fig. 4), we have got elaborate the 5-docked protein and ligand composite with the hydrogen bond contacts as well as the superimposition of the ligands within the binding pocket (Vyas et al., 2013). After MD simulations, re-docked all five compounds with VP-3. The re-docked results revealed that all five compounds increased their binding affinity without alterations in active site residues Table 1. The five lead ligands were also bound inside the active site of the similar pose. They were occupied the S1, S2, S3 sub-sites (Fig. S4). The MD simulation is a procedure methodology analyses the instance reliant behaviour of a molecular co-ordination. MD simulations encompass Safford elaborate data on the fluctuations and conformational alterations of protein and nucleic acids. These ways are currently habitually accustomed consider the configuration, dynamics as well as thermodynamics of organic compounds along with their complexes. They're conjointly employed in the purpose of structures from x-ray crystallography plus from MR (magnetic resonance) research. The MD simulation revisions were executed to investigate the reliability of the macromolecule by NAMD tool 2.7. The basis root means square deviation (RMSD) enhanced at the start of the simulation. It is a frequently used measure of the differences between two superimposed atomic coordinates score is 1.44 Å. The predicted by a model or an estimator and the values observed. RMSD can be calculated for any type and subset of atoms; for example, Cα atoms of the entire protein, Cα atoms of all residues in a specific subset of a protein. And the RMSD usually requires careful consideration of internal symmetry where the atom pair correspondence in atoms within each structure which are topologically equivalent to one

Table 1. Leupeptin and its analogs along with their respective interaction residues and AutoDock binding energies before and after MD simulations.

Compound PubChem ID	No. of H-bonds	Before simulation	After simulation	Active site amino acids
		AutoDock binding affinity (ΔGb) k.cal/mol		
CID74427946	5	−10.8	−12.0	GLY-85, HIS-176, SER-151, GLN-236
CID74427945	5	−10.2	−11.1	ASN-86, GLY-85, HIS-176
CID 360883	5	−9.7	−10.6	ILE-87, ASN-86, GLY-85, ASN-175, GLN-236
CID 193721	6	−9.2	−10.0	SER-151, GLN236, ASN-86, GLY-85
CID 51416859	6	−8.9	−9.8	ASN-86, GLY-85, ASN-175
CID 72429 (Query)	7	−6.5	−	GLY-85, ASN-86, SER-151, HIS-176

https://doi.org/10.1016/j.heliyon.2018.e00612

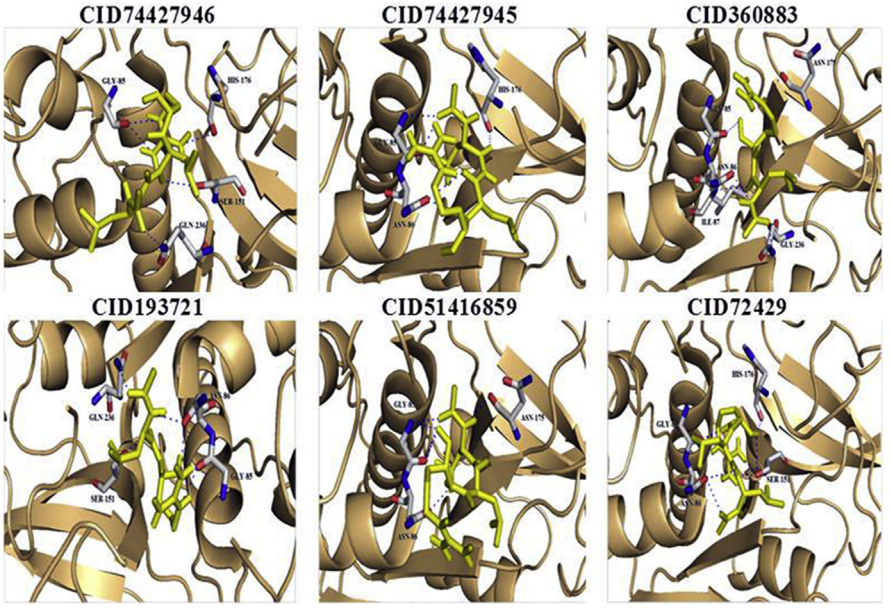

Fig. 4. Interactions of respective Leupeptin (CID72429) and its analogs with *Plasmodium vivax* VP-3 model. Ligands are shown colored (yellow) by atom type whereas protein residues nearby were shown in color sticks. Hydrogen bonding interactions were shown in blue color dots.

another. MD simulations is nothing but physical movements of atoms and molecules in confined boundary surface. The atoms and molecules can interact for a fixed period of time, giving a view of the dynamic evolution of the system. The trajectories of the atoms and molecules are determined Newton's equations of motion. Molecular dynamics simulations permit the study of complex, dynamic processes that occur in biological systems implies the protein stability, conformational changes, protein folding, molecular recognition. The designed VP-3 had a stumpy RMSD charge (0.2−0.3 Å) for the stamina, that designate steadiness as well as a constant forceful behaviour of the VP-3. The MD simulation revision illustrated that the power of the compound was constant all over the simulation phase. The simulation revision conjointly signify that the stamina RMSD improved between 5 ns and 15 ns, and it had been steady for the remainder of the phase of the simulation, and the VP-3 was quite stable after 15 ns up to 20 ns (Fig. 5).

The predicted model of VP-3 from *Plasmodium vivax* was focused to MD simulation to determine the steadiness of leads in the active site of VP-3. MD simulation study for 20 ns was performed for the VP-3 protein in explicit water. MD simulations compute steadiness of the docked conformations. The five different docked complexes (VP-3_74427945, VP-3_74427946, VP-3_360883, VP-3_51416859 and VP-3_193721) were subjected to 20 ns of MD simulation (Fig. 6). The calculation of binding free energy and hydrogen bond interaction analysis of these five compounds will deliver the detailed evidence about the alterations of the target molecules. All the five compounds have showed similar VP-3 inhibitory activity

https://doi.org/10.1016/j.heliyon.2018.e00612

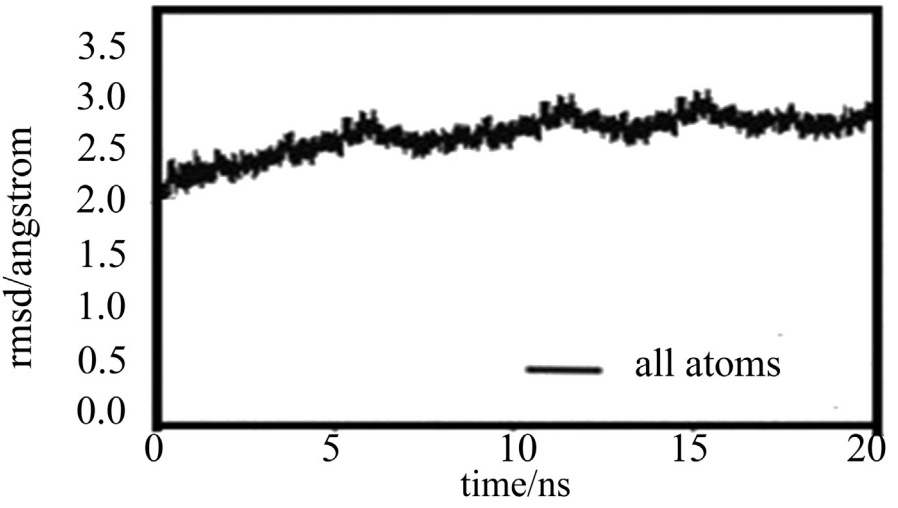

Fig. 5. The RMSD peaks of the all atoms of the modeled protein (VP-3) over a period of 20 ns.

with leupeptin. Although all molecules were bound to the hemoglobin pocket, and extended to solvent regions in diverse directions. In order to comprehend the effect on selectivity with different extending directions, MD simulation, hydrogen bond habitation and binding free energy calculations were conjointly achieving on the protein−small molecules complexes (Nanda Kumar et al., 2017). To explore the dynamic steadiness of the co-ordination, RMSD analysis using the beginning structure used as reference were calculated. In the process of a 20 ns MD simulation on VP-3 in complex with all five compounds, both protein and ligands RMSD plots clearly indicated that some fluctuation at the beginning, but the overall actual values were very nearer. The protein receptor of backbone fluctuated in the range of 2−2.5 Å, and a ligand changed in the range of 1.25−1.05 Å, indicating the system stayed in an equilibrated and converged stage and kept stable. No changes were found in the conserved amino acids in the process of the simulation, like the active site region (Gly-85, Asn-86, Ile-87, Ser-151, Asn-175, His-176 and Gln-236) indicating that the ligand binding site was also kept in a stable confirmation. The fluctuation the protein considering the RMSD values shown in (Fig. 6). The ligand binding free energy were calculated for the two compounds using MM/PBSA and MM/GBSA methods (Table. S2) respectively. The binding free energy was measured to reflect the binding affinity of the ligands. All the five compounds got more favorable ΔPBTOT and ΔGBTOT values, indicating five compounds got higher binding energies with binding pocket (Cunha et al., 2004). In view of all the above results, five compounds got almost the same interactions with the VP-3 (Fig. 4). Consequently, the structural optimization in the protein hydrogen bond rich region may be a reasonable solution to improve VP-3 inhibitory activity.

https://doi.org/10.1016/j.heliyon.2018.e00612

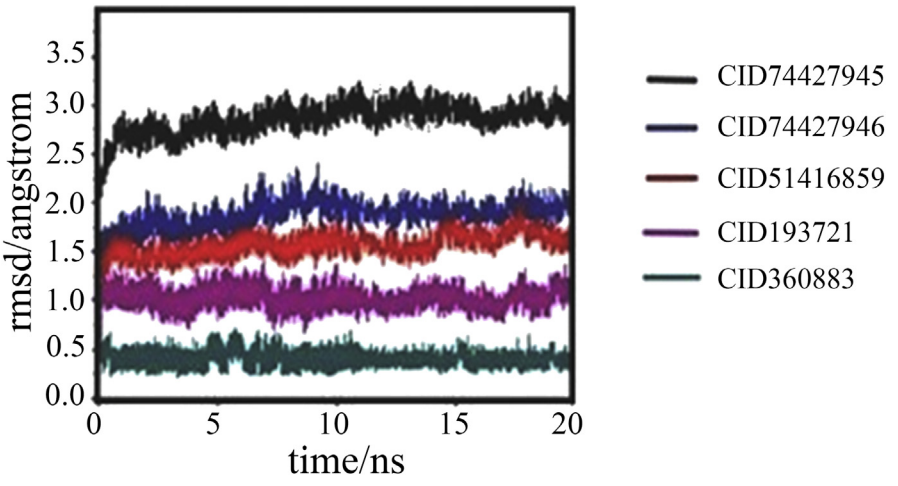

Fig. 6. The RMSD of the selected five ligands CID74427945, CID74427946, CID51416859, CID193721, CID360883 in the active site of VP-3.

3.5. Ligand validations and drug-likeness

All the molecules were analyzed for Lipinski "Rule of five" i.e., "drug-likeness". The compounds showed *Log P* $\leq$ 5, relative molecular mass $\leq$500, range of HBA (hydrogen bond acceptors) $\leq$10, and range of HBD (hydrogen bond donors) $\leq$5 considered as best ligand molecules used as drug leads for biological activity (Table 2). Lipinski's rule of five could be a law of thumb designed for evaluating the drug likeness, or deciding if a substance through a particular pharmacologic or biological actions that may possibly create it a credible verbally energetic compound in humans. The results showed that five best lead molecules, i.e., CID 74427945, CID 74427946, CID 360883, CID193721 and CID 51416859 fulfilled the "Rule of 5" (Fig. 7). The drug-likeness properties of all these compounds are showing in the (Table 2).

3.6. ADME predicting activity

The Lipinski "Rule of 5" revealed the molecular properties crucial for a drug's pharmacology contained by the investigation, collectively with its ADME, it doesn't envisage if a molecule is pharmacologically dynamic. For that reason, pharmacokinetic properties and toxicities were foretold for every one of the five compounds used by OSIRIS property explorer server. Outcome of pharmacokinetic properties and toxicity investigation are revealed within the (Table 3). The solubility and partition coefficient were proposed for pharmacology possessions, although tumorigenicity, mutagenicity, irritation force and hazard of reproductive force was foretold for toxicity revision. On the way to exertion exposed the hydrophilicity, *log P* value was foretold. It's reminiscent that a lofty *log P* value is correlated to pitiable absorption or penetration and it should be but five (Guimaraes et al., 2011). Outcome

https://doi.org/10.1016/j.heliyon.2018.e00612

Table 2. Different physicochemical parameters/properties contributing the drug score by MolSoft drug likeness tool. *MF- Molecular formula, MW- Molecular weight, HBA- Hydrogen bond acceptor, HBD- Hydrogen bond donor, PSA- Polar surface area, Mol Vol- Molecular volume.

Properties	CID74427946	CID74427945	CID360883	CID193721	CID51416859
MF*	$C_{20}H_{38}N_6O_4$	$C_{20}H_{39}N_6O_4$	$C_{14}H_{27}N_5O_3$	$C_{14}H_{27}N_5O_3$	$C_{20}H_{39}N_6O_4$
MW*	426.30	427.30	313.21	314.32	421.30
No. of HBA*	5	5	4	4	4
No. of HBD*	7 (>5)	8 (>5)	6 (>5)	6 (>5)	8 (>5)
Mol LogP	−0.25	−0.98	−0.28	−0.27	−0.19
Mol LogS	−3.76	−3.76	−2.43	−2.45	−3.76
Mol PSA* (moles/L)	$137.22A^2$	$137.22A^2$	$112.91A^2$	$113.21A^2$	$137.22A^2$
Mol Vol*	$452.55A^3$	$446.95A^3$	$328.01A^3$	$328.01A^3$	$448.81A^3$
No. of stereo centres	3	3	2	2	3
Drug likeness model score	−0.21	−0.30	−0.59	−0.58	−0.69

exposed that everyone the five compounds recognized to the existing boundary as well as among the five compounds, CID74427946 have a significantly improved *clog P* value than others (Table 3). In general, a pitiable solubility is consistent to perilous absorption and the liquid solubility (*log S*) of a compound noticeably affects its absorption and distribution quality. Results showed that CID360883 encompasses an elevated *log S* value than others (Table 2). Accordingly, as to consider the compound's overall prospective as a drug candidate, drug score is also deliberate which mixes drug likeness, *clog P, TPSA*, relative molecular weight, and toxicity

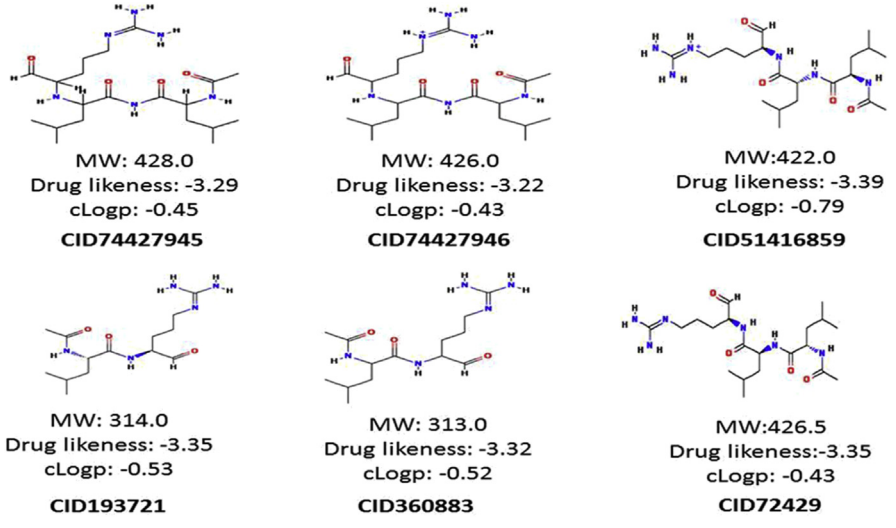

Fig. 7. Best five ligand CID74427945, CID74427946, CID51416859, CID193721, CID360883 of VP-3 model.

https://doi.org/10.1016/j.heliyon.2018.e00612

Table 3. *In silico* ADMET prediction by OSIRIS property explorer.

Properties	CID74427946	CID74427945	CID360883	CID193721	CID51416859
Mutagenic	No	No	No	No	No
Tumorigenic	No	No	No	No	No
Irritant	No	No	No	No	No
Reproductive effective	No	No	No	No	No
C Log p	−0.43	−0.45	−0.52	−0.53	−0.79
Solubility	−3.24	−3.28	−2.38	−2.39	−2.14
MW	426.0	428.0	313.0	314.0	422.0
TPSA	168.7	165.2	139.1	139.6	162.5
Drug likeness	−3.22	−3.29	−3.32	−3.35	−3.39
Drug score	0.41	0.43	0.45	0.47	0.41

risk parameters as publicized within the (Table 3). The drug score showed that the compounds, CID193721 and CID360883, have higher scores of 0.47 and 0.45 contrast to the others.

3.7. Antimalarial activity

The antimalarial screening results of test compounds, against *P. vivax* at 10, 20, 50, and 100μM concentrations and Leupeptin as reference drug. It was observed that the all test compounds displayed killing of parasitemia ranging from 26.2−37.3% at 10 μM, 41.5−58.4% at 20 μM, 52.5−64.7% at 50 μM and 69.7−82.6% at 100 μM were reported against *P. vivax*. Results revealed that among the all compounds CID74427946 (82.6 ± 1.2), CID74427945 (79.5 ± 0.7) and CID360883 (75.3 ± 1.0) were showed the highest activity against *P. vivax*. The rest of compounds were also showed good activity than the reference drug (Fig. 8).

The antimalarial activity (IC_{50}) of all test compounds compared to Leupeptin as a common antimalarial drug was presented in (Fig. 8). Compound CID74427946 (1.0 ± 0.35), CID74427945 (1.5 ± 0.24) and CID360883 (2.1 ± 0.45) were revealed to that IC_{50} were greater than the reference drug. Keeping the all above results indicated that the compounds CID74427946, CID 74427945 and CID360883 were showed best killing of parasitemia activity.

3.8. Cytotoxicity assay

MTT cell based assays often used for validating screening cytotoxicity for collections of compounds. The set of test compounds were validating by setting at different concentrations 20−100 μg/ml. The ligand drugs are supposed administered as a solution in DMSO and DMSO + control. The proposed ligand leads showed good cytotoxic behavior and can considered being potent cytotoxic agents. The results

https://doi.org/10.1016/j.heliyon.2018.e00612

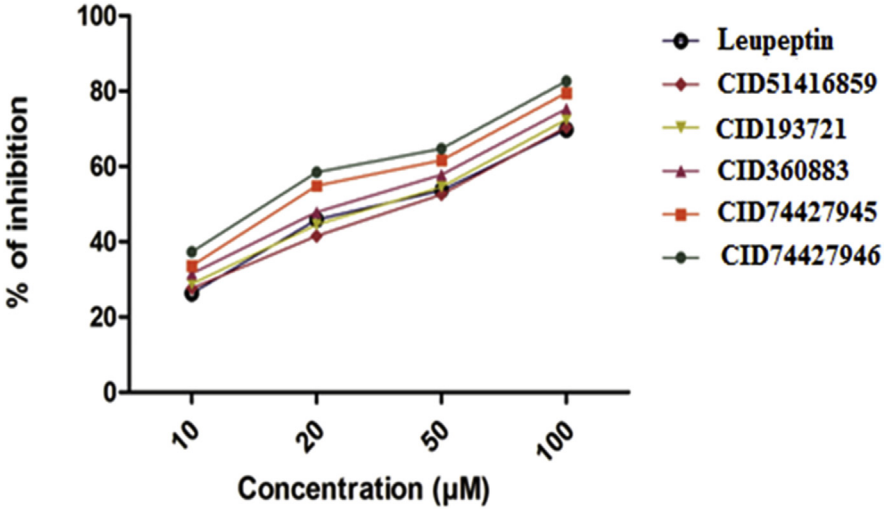

Fig. 8. Antimalarial activity of CID74427946, CID74427945, CID360883, CID193721, CID51416859 and Leupeptin compounds against *P. vivax.*

show that cell viability decreased with increase in concentration with 20−100 µg/mL. All test ligand compounds showed significant concentration in dependent cytotoxicity. Based on the cytotoxicity assay results the potent compounds were screened for against rat PC12 (Pheochromocytoma) cell lines using standard drug. *In vitro* growth effect of test compounds revealed that compounds CID74427946, CID74427945 and CID360883 were exhibited good potential cytotoxicity (Fig. 9). The higher activity of compounds CID74427946, CID74427945 and CID360883 were also correlation above studies.

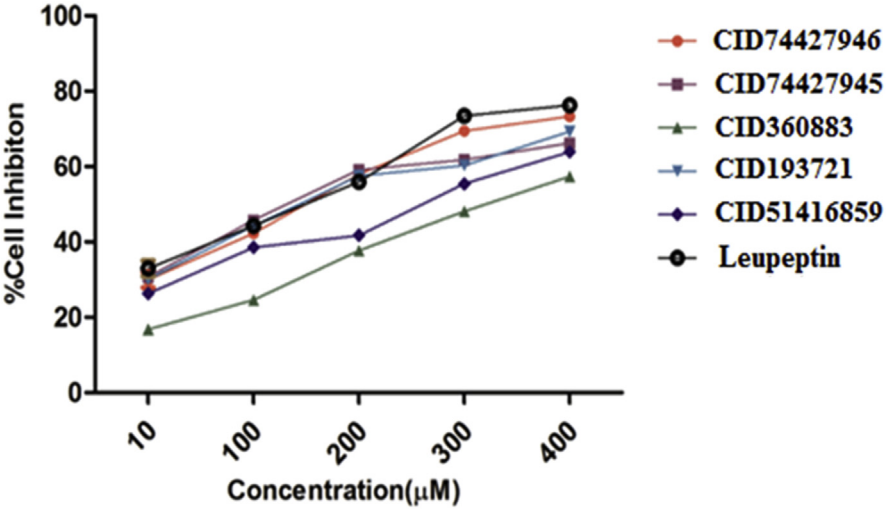

Fig. 9. Cytotoxicity in PC12 (pheochromocytoma) cells for compounds CID74427946, CID74427945, CID360883, CID193721, CID51416859 and Leupeptin.

https://doi.org/10.1016/j.heliyon.2018.e00612

4. Conclusions

A structure-based pharmacophore was produced supported the intricate structure of VP-3 and leupeptin. The created pharmacophore model was utilized for the screening of known hits were further assessed by molecular docking, MD simulation and binding affinity expectation. Therefore, five lead hits were accounted for that fulfilled every one of the benchmarks for the arranging of compounds that may demonstration about as great leads for the occasion of new, attractive and basically different compounds for VP-3 inhibition. The ligand pairing mode, anticipated by docking, it had been discovered that there are some particular functional groups that copy the combination mode of Leupeptin into an active site location of VP-3. The five leads conjointly demonstrated the best affinity among screened compounds. The MD simulations for the VP-3 five lead compounds were performed to acknowledge conformational stability, structural flexibility as well as molecular dynamics of the collaboration in physiological condition. All the ligands are entirely steady inside the position of VP-3 active site. The important role of the five compounds increased their binding affinity without alterations in active site residues of the pathologic enzyme VP-3. The evaluation of antimalarial activity and cytotoxicity activity results were also support the above studies. In the modulations both *in vitro* and *in vivo*, with conceivable and potential implications in a new therapeutic approach in malaria drug discovery.

Declarations

Author contribution statement

Madhu Sudhana Saddala: Performed the experiments; Analyzed and interpreted the data; Contributed reagents, materials, analysis tools or data; Wrote the paper.

Pradeepkiran Jangampalli Adi: Conceived and designed the experiments; Analyzed and interpreted the data; Contributed reagents, materials, analysis tools or data; Wrote the paper.

Funding statement

This research did not receive any specific grant from funding agencies in the public, commercial, or not-for-profit sectors.

Competing interest statement

The authors declare no conflict of interest.

https://doi.org/10.1016/j.heliyon.2018.e00612

Additional information

Supplementary content related to this article has been published online at https://doi.org/10.1016/j.heliyon.2018.e00612.

Acknowledgements

We are very thankful to the reviewers and editor for providing valuable suggestions to improve the manuscript, we also thank our lab mates who encouraged us to carry out this work.

References

Altschul, S.F., Madden, T.L., Schäffer, A.A., Zhang, J., Zhang, Z., Miller, W., Lipman, D.J., 1997. Gapped BLAST and PSI-BLAST: a new generation of protein database search programs. Nucleic Acids Res. 25, 3389−3402.

Berendsen, H.J.C., Postma, J.P.M., Vangunsteren, W.F., DiNola, A., Haak, J.R., 1984. Molecular-dynamics with coupling to an external baths. J. Chem. Phys. 81, 3684−3690.

Bonilla, J.A., Bonilla, T.D., Yowell, C.A., Fujioka, H., Dame, J.B., 2007a. Critical roles for the digestive vacuole plasmepsins of *Plasmodium falciparum* in vacuolar function. Mol. Microbiol. 65, 64−75.

Bonilla, J.A., Moura, P.A., Bonilla, T.D., Yowell, C.A., Fidock, D.A., Dame, J.B., 2007b. Effects on growth, hemoglobin metabolism and paralogous gene expression resulting from disruption of genes encoding the digestive vacuole plasmepsins of *Plasmodium falciparum*. Int. J. Parasitol. 37, 317−327.

Bowie, J.U., Luthy, R., Eisenberg, D., 1991. A method to identify protein sequences that fold into a known three-dimensional structure. Science 253, 164−170.

Brooks, B.R., Bruccoleri, R.E., Olafson, B.D., States, D.J., Swaminathan, S., Karplus, M., 1983. A program for macromolecular energy, minimization, and dynamics calculations. J. Comput. Chem. 4, 187−217.

Carlton, J., 2003. The *Plasmodium vivax* genome sequencing project. Trends Parasitol. 19, 227−231.

Colovos, C., Yeates, T.O., 1993. Verification of protein structures: patterns of nonbonded atomic interactions. Protein Sci. 2, 1511−1519.

Cunha, E.F.F.D., Ramalho, T.C., Alencastro, R.B.D., Maia, E.R., 2004. Interactions of 5-deazapteridine derivatives with *Mycobacterium tuberculosis* and with human dihydrofolate reductases. J. Biomol. Struct. Dyn. 22, 119−130.

Dallakyan, S., 2008. PyRx-Python Prescription v.0.8. The Scripps Research Institute, La Jolla.

Darden, T., York, D., Pedersen, L., 1993. Particle mesh Ewald: an N·log(N) method for Ewald sums in large systems. J. Chem. Phys. 98, 10089−10092.

Dolly, A., Griffiths, J.B., 2000. Cell and Tissue Culture for Medical Research. John Wiley & Sons, ISBN 978-0-471-85213-1, pp. 1−468.

Eggleson, K.K., Duffin, K.L., Goldberg, D.E., 1999. Identification and characterization of falcilysin, a metallopeptidase involved in hemoglobin catabolism within the malaria parasite *Plasmodium falciparum*. J. Biol. Chem. 274, 32411−32417.

Eswar, N., Eramian, D., Webb, B., Shen, M.Y., Sali, A., 2008. Protein structure modeling with MODELLER. Meth. Mol. Biol. 426, 145−159.

Francis, S.E., Sullivan, D.J., Goldberg, D.E., 1997. Hemoglobin metabolism in the malaria parasite *Plasmodium falciparum*. Annu. Rev. Microbiol. 51, 97−123.

Fryauff, D.J., Tuti, S., Mardi, A., Masbar, S., Patipelohi, R., Leksana, B., Kain, K.C., Bangs, M.J., Richie, T.L., Baird, J.K., 1998. Chloroquine-resistant *Plasmodium vivax* in transmigration settlements of west Kalimantan, Indonesia. Am. J. Trop. Med. Hyg. 59, 513−518.

Gluzman, I.Y., Francis, S.E., Oksman, A., Smith, C.E., Duffin, K.L., Goldberg, D.E., 1994. Order and specificity of the *Plasmodium falciparum* hemoglobin degradation pathway. J. Clin. Invest. 93, 1602−1608.

Guimaraes, A.P., Oliveira, A.A., Cunha, E.F.F.D., Ramalho, T.C., França, T.C., 2011. Analysis of *Bacillus anthracis* nucleoside hydrolase via in silico docking with inhibitors and molecular dynamics simulation. J. Biomol. Struct. Dyn. 17, 2939−2951.

Humphrey, W., Dalke, A., Schulten, K., 1996. VMD: visual molecular dynamics. J. Mol. Graph. Model. 14, 27−28.

Izaguirre, J.A., Catarello, D.P., Wozniak, J.M., Skeel, R., 2001. Langevin stabilization of molecular dynamics. J. Chem. Phys. 114, 2090−2098.

Jorgensen, W.L., Chandrasekha, J., Madura, J.D., 1983. Comparison of simple potential functions for simulating liquid water. J. Chem. Phys. 79, 926−935.

Laskowski, R.A., MacArthur, M.W., Moss, D.S., Thornton, J.M., 1993. PROCHECK: a program to check the stereochemical quality of protein structures. J. Appl. Crystallogr. 26, 283−291.

Laxmikant, K., Robert, S., Milind, B., Robert, B., Attila, G., Neal, K., 1999. NAMD2: greater scalability for parallel molecular dynamics. J. Chem. Phys. 151, 283−312.

https://doi.org/10.1016/j.heliyon.2018.e00612

Leeson, P., 2012. Drug discovery: chemical beauty contest. Nature 481, 455–456.

Lipinski, C.A., Lombardo, F., Dominy, B.W., Feeney, P.J., 1997. Experimental and computational approaches to estimate solubility and permeability in drug discovery and development settings. Adv. Drug Deliv. Rev. 23, 3–25.

Luthy, R., Bowie, J.U., Eisenberg, D., 1992. Assessment of protein models with three-dimensional profiles. Nature 356, 83–85.

MacKerell, A.D., Bashford, D., Bellott, M., Dunbrack, R.L., Evanseck, J.D., Field, M.J., Fischer, S., Gao, J., Guo, H., Ha, S., Joseph-McCarthy, D., Kuchnir, L., Kuczera, K., Lau, F.T., Mattos, C., Michnick, S., Ngo, T., Nguyen, D.T., Prodhom, B., Reiher, W.E., Roux, B., Schlenkrich, M., Smith, J.C., Stote, R., Straub, J., Watanabe, M., Wiórkiewicz-Kuczera, J., Yin, D., Karplus, M., 1998. All-atom empirical potential for molecular modeling and dynamics studies of proteins. J. Phys. Chem. B 102, 3586–3616.

Maes, K., Testelmans, D., Powers, S., Decramer, M., Gayan-Ramirez, G., 2007. Leupeptin inhibits ventilator-induced diaphragm dysfunction in rats. Am. J. Respir. Crit. Care Med. 175, 1134–1138.

Morris, G.M., Huey, R., Lindstrom, W., Sanner, M.F., Belew, R.K., Goodsell, D.S., Olson, A.J., 2009. AutoDock4 and AutoDockTools4: automated docking with selective receptor flexibility. J. Comput. Chem. 30, 2785–2791.

Na, B.K., Shenai, B.R., Sijwali, P.S., Choe, Y., Pandey, K.C., Singh, A., Craik, C.S., Rosenthal, P.J., 2004. Identification and biochemical characterization of vivapains, cysteine proteases of the malaria parasite *Plasmodium vivax*. Biochem. J. 378, 529–538.

Naing, C., Whittaker, M.A., Wai, V.N., Mak, J.W., 2014. Is *Plasmodium vivax* malaria a severe malaria? A systematic review and meta-analysis. PLoS Negl. Trop. Dis. 8, e3071.

Nanda Kumar, Y., Kalpana, K., Ramesh, K., Pradeepkiran, J.A., 2017. Conformational transition pathway of R308K mutant glucokinase in presence of the glucokinase activator YNKGKA4. FEBS Open Bio.

Pradeepkiran, J.A., Kumar, K.K., Kumar, Y.N., Bhaskar, M., 2015. Modeling, molecular dynamics, and docking assessment of transcription factor rho: a potential drug target in *Brucella melitensis* 16M. Drug Des. Dev. Ther. 9, 1897–1912.

Phillips, J.C., Braun, R., Wang, W., Gumbart, J., Tajkhorshid, E., Villa, E., Chipot, C., Skeel, R.D., Kalé, L., Schulten, K., 2005. Scalable molecular dynamics with NAMD. J. Comput. Chem. 26, 1781–1802.

https://doi.org/10.1016/j.heliyon.2018.e00612

Rawat, M., Vijay, S., Gupta, Y., Tiwari, P.K., Sharma, A., 2011. Sequence homology and structural analysis of plasmepsin 4 isolated from Indian *Plasmodium vivax* isolates. Infect. Genet. Evol. 11, 924–933.

Reblova, K., Lankas, F., Razga, F., Krasovska, M.V., Koca, J., Sponer, J., 2006. Structure, dynamics, and elasticity of free 16s rRNA helix 44 studied by molecular dynamics simulations. Biopolymers 82, 504–520.

Rieckmann, K.H., Sax, L.J., Campbell, G.H., Mrema, J.E., 1978. Drug sensitivity of *Plasmodium falciparum*. An in-vitro microtechnique. Lancet 1, 22–23.

Ross, W.S., Hardin, C.C., 1994. Ion-induced stabilization of the G-DNA Quadruplex: free energy Perturbation studies. J. Am. Chem. Soc. 116, 6070–6080.

Ruebush, T.K., Zegarra, J., Cairo, J., Andersen, E.M., Green, M., Pillai, D.R., Marquiño, W., Huilca, M., Arévalo, E., Garcia, C., Solary, L., Kain, K.C., 2003. Chloroquine resistant *Plasmodium vivax* malaria in Peru. Am. J. Trop. Med. Hyg. 69, 548–552.

Ryckaert, J.P., Ciccotti, G., Berendsen, H.J.C., 1977. Numerical integration of the Cartesian equations of motion of a system with constraints: molecular dynamics of n-alkanes. J. Comput. Phys. 23, 327–341.

Shenai, B.R., Sijwali, P.S., Singh, A., Rosenthal, P.J., 2000. Characterization of native and recombinant falcipain-2, a principal trophozoite cysteine protease and essential hemoglobinase of *Plasmodium falciparum*. J. Biol. Chem. 275, 29000–29010.

Sijiwali, P.S., Shenai, B.R., Gut, J., Singh, A., Rosenthal, P.J., 2001. Expression and characterization of the *Plasmodium falciparum* haemoglobinase falcipain-3. Biochem. J. 489, 481–489.

Sippl, M.J., 1993. Recognition of errors in three-dimensional structures of proteins. Proteins 17, 355–362.

Spackova, N., Sponer, J., 2006. Molecular dynamics simulations of sarcin-ricin rRNA motif. Nucleic Acids Res. 34, 697–708.

Thompson, J.D., Gibson, T.J., Plewniak, F., Jeanmougin, F., Higgins, D.G., 1997. The CLUSTAL_X windows interface: flexible strategies for multiple sequence alignment aided by quality analysis tools. Nucleic Acids Res. 24, 4876–4882.

Trager, W., Jensen, J.B., 1976. Quantitative dissection of clone-specific growth rates in cultured malaria parasites. Science 193, 673–685.

https://doi.org/10.1016/j.heliyon.2018.e00612

Vyas, V.K., Ghate, M., Goel, A., 2013. Pharmacophore modeling, virtual screening, docking and in silico ADMET analysis of protein kinase B (PKB β) inhibitors. J. Mol. Graph. Model. 42, 17−25.

Wiederstein, M., Sippl, M.J., 2007. ProSA-web: interactive web service for the recognition of errors in three-dimensional structures of proteins. Nucleic Acids Res. 35, W407−W410.

Wolber, G., Langer, T., 2005. LigandScout: 3-D pharmacophores derived from protein-bound ligands and their use as virtual screening filters. J. Chem. Inf. Model. 45, 160−169.

 https://doi.org/10.1016/j.heliyon.2018.e00612